Published in final edited form as:
Eur J Neurosci. 2013 November ; 38(9): 3314–3324. doi:10.1111/ejn.12337.

Traits of fear resistance and susceptibility in an advanced intercross line

Jennifer L. McGuire[1], **Hadley C Bergstrom**[1,2], **Clarissa C. Parker**[3], **Thien Le**[1,2], **Maria Morgan**[1], **Haiying Tang**[4], **Reed Selwyn**[4], **Afonso C. Silva**[5], **Kwang Choi**[1,2], **Robert J. Ursano**[1,2], **Abraham A. Palmer**[3,6], and **Luke R. Johnson**[1,2,7]

[1]Department of Psychiatry and Program in Neuroscience, Uniformed Services University (USU), School of Medicine, Bethesda, MD, USA

[2]Center for the Study of Traumatic Stress (CSTS)

[3]Department of Human Genetics, University of Chicago, IL, USA

[4]Department of Radiology, Uniformed Services University (USU), School of Medicine, Bethesda, MD, USA

[5]National Institute of Neurological Disorders and Stroke, National Institutes of Health, Bethesda, MD, USA

[6]Department of Psychiatry and Behavioral Neuroscience, University of Chicago, IL, USA

[7]Translational Research Institute (TRI), Institute for Health and Biomedical Innovation (IHBI), Department of Psychology, Queensland University of Technology (QUT), Brisbane, Qld, 4059, Australia

Abstract

Genetic variability in the strength and precision of fear memory is hypothesized to contribute to the etiology of anxiety disorders, including post-traumatic stress disorder. We generated fear-susceptible (F-S) or fear-resistant (F-R) phenotypes from an F_8 advanced intercross line (AIL) of C57BL/6J and DBA/2J inbred mice by selective breeding. We identified specific traits underlying individual variability in Pavlovian conditioned fear learning and memory. Offspring of selected lines differed in the acquisition of conditioned fear. Furthermore, F-S mice showed greater cued fear memory and generalized fear in response to a novel context than F-R mice. F-S mice showed greater basal corticosterone levels and hypothalamic corticotrophin-releasing hormone (CRH) mRNA levels than F-R mice, consistent with higher hypothalamic–pituitary–adrenal (HPA) axis drive. Hypothalamic mineralocorticoid receptor and CRH receptor 1 mRNA levels were decreased in F-S mice as compared with F-R mice. Manganese-enhanced magnetic resonance imaging (MEMRI) was used to investigate basal levels of brain activity. MEMRI identified a pattern of increased brain activity in F-S mice that was driven primarily by the hippocampus and amygdala,

Correspondence: Dr Luke R. Johnson, [7]Translational Research Institute, as above. LukeJohnsonPhD@gmail.com.

Aspects of this work were presented at the Society for Neuroscience Annual Meeting, 14 October 2012, the Amygdala, Stress and PTSD Conference, 24 April 2012, and in the following *Nature News* article: Stress: the roots of resilience. *Nature* 490, 165–167 (11 October 2012), http://www.nature.com/news/stress-the-roots-of-resilience-1.11570.

The authors declare no conflicts of interest.

indicating excessive limbic circuit activity in F-S mice as compared with F-R mice. Thus, selection pressure applied to the AIL population leads to the accumulation of heritable trait-relevant characteristics within each line, whereas non-behaviorally relevant traits remain distributed. Selected lines therefore minimize false-positive associations between behavioral phenotypes and physiology. We demonstrate that intrinsic differences in HPA axis function and limbic excitability contribute to phenotypic differences in the acquisition and consolidation of associative fear memory. Identification of system-wide traits predisposing to variability in fear memory may help in the direction of more targeted and efficacious treatments for fear-related pathology.

Keywords

AIL; amygdala; fear conditioning; fear generalization; hippocampus; HPA axis; manganese-enhanced MRI

Introduction

Learning about and remembering fearful experiences is critical to survival. Disturbances in this fundamental behavior are linked to a variety of psychiatric diagnoses. Stronger acquisition of conditioned fear is a common trait among patients with anxiety disorders, including post-traumatic stress disorder (PTSD) and depression (Orr *et al.*, 2000; Lissek *et al.*, 2005; Nissen *et al.*, 2010; Norrholm *et al.*, 2011). PTSD in particular is associated with dysregulation of fear memory circuits (Tryon, 1999; Elzinga & Bremner, 2002; Shin & Handwerger, 2009). Pavlovian fear conditioning is a robust and well-established paradigm for studying emotional memory in both humans and animals (Orr *et al.*, 2000; Amstadter *et al.*, 2009; Johnson *et al.*, 2012; Mahan & Ressler, 2012). Importantly, individual variability in 'conditionability', or the strength of memory formation, is heritable (Hettema *et al.*, 2003; Johnson *et al.*, 2012). Thus, identifying biological traits predicting fear memory formation has important clinical implications for both understanding the etiology of, and developing intervention strategies for, disorders of fear regulation (Shin & Handwerger, 2009; Johnson *et al.*, 2012).

Selective breeding has been used in behavioral genetics for decades (Hall, 1938). Genetically heterogeneous populations are necessary for selective breeding. A simple and well-defined outbred population is an advanced intercross line (AIL). AILs are created through pseudo-random breeding over multiple generations, reducing the linkage of nearby alleles (Parker & Palmer, 2011). In this study, we used three generations of bi-directional selective breeding for contextual fear memory to establish two divergent lines, which we call fear-susceptible (F-S) and fear-resistant (F-R). We then examined physiological and neural traits in behaviorally naïve mice whose parents were from the final selected generation. These included parametric study of fear conditioning, baseline hypothalamic–pituitary–adrenal (HPA) axis function, HPA axis gene expression, and measures of brain structure and function *in vivo* with manganese-enhanced magnetic resonance imaging (MEMRI). MEMRI signal enhancement primarily derives from intracellular accumulation of Mn^{2+} through voltage-gated Ca^{2+} channels, allowing high-resolution visualization of functionally

dependent neural processing and brain anatomy (Koretsky, 2004; Silva *et al.*, 2004; Silva & Bock, 2008; Koretsky, 2012).

We are using a carefully designed AIL with short-term selection to segregate trait-relevant allelic combinations with minimal random genetic drift (Belknap *et al.*, 1997). This strategy greatly reduces potential non-specific contributions of the genetic background, and increases the likelihood that divergence between lines relates directly to the selection criterion. A major strength of our behavioral selection strategy is that we were able to evaluate these phenotypes in behaviorally naïve animals, and thus we can identify genetically determined physiological profiles that may contribute to the differences in strength of fear memory encoding. Identification of a physiological profile of fear resistance and susceptibility is a key milestone in identifying endophenotypes of altered fear memory processing and ultimately a biological basis for PTSD and other anxiety disorders.

Materials and methods

Subjects

Mouse lines were derived from the F_8 generation of a C57BL/6J × DBA/2J AIL created by Palmer (Parker *et al.*, 2012). F_8 AIL mice were trained and tested for cued and contextual fear in a Pavlovian fear conditioning protocol in Chicago, as described previously (Ponder *et al.*, 2007; Parker *et al.*, 2012). Mice showing either the highest or lowest contextual fear [selected generation 1 (S1)] were assigned into breeding pairs and shipped to the Uniformed Services University of the Health Sciences (USUHS) laboratory animal facility. Breeding and selection of successive generations [selected generation 2 (S2) and selected generation 3 (S3)] was conducted at USUHS. Mice were housed two to five per cage in a climate-controlled vivarium on a 12 : 12-h light cycle (lights on 06:00 h) with *ad libitum* access to food and water. Experiments were conducted in accordance with the National Institutes of Health *Guide for the Care and Use of Animals.* All experimental procedures were reviewed and approved by the appropriate (University of Chicago or USUHS) Institutional Care and Use Committee.

Behavioral phenotyping

F-R and F-S mice, 8–12 weeks old, were tested for contextual and cued conditioned fear response with a fear conditioning protocol described previously and below (Ponder *et al.*, 2007) (Fig. 1A). Freezing was scored with ANYMAZE analysis software (Stoelting, Wood Dale, IL, USA). The selection criterion was the percentage of freezing during the first 300 s or the contextual fear test. F-S mice with the highest freezing and F-R mice with the lowest freezing were retained for breeding, and paired according to their freezing scores. To maintain heterogeneity, related mice were not paired for breeding. We used mass selection, meaning that we did not place limits on how many mice were selected from each family to breed the next generation. Two or three litters per breeding pair were phenotyped, to increase the likelihood that the majority of breeding pairs would be represented in the subsequent generation.

In S1, 118 mice were phenotyped and 60 mice were selected to create 15 F-R and 15 F-S breeding pairs (~50% of the total S1 cohort). Three hundred and forty-eight mice (150 F-S and 198 F-R) were phenotyped in S2 to establish 11 F-S and 12 F-R breeding pairs (~15% of each cohort in S2). Two hundred and thirty mice were phenotyped in S3 (134 F-S and 98 F-R). Fifteen F-S and 15 F-R breeding pairs were established from the S3 litters (25–30% of each cohort in S3).

Phenotyping was performed over a period of 3 days (Fig. 1A): training on day 1, context fear test on day 2, and cued fear test on day 3. Training consisted of a 3-min exploration period followed by two presentations of a 30-s, 4.5-kHz, 75-dB pure tone conditioned stimulus (CS) co-terminating in a 2-s, 0.5-mA foot shock delivered with a 30-s interval through a conducting floor. On day 2, the mice were returned to the training chamber for 600 s. The first 300 s were scored for context-related fear. On day 3, the chamber was altered for visual, tactile and olfactory cues. House lights in the chamber were turned up and filtered through a yellow filter. The conducting rods were covered with smooth plastic, and patterned inserts covered the chamber walls. The cleaning solution was changed from 70% ethanol to 1% acetic acid. After 3 min of exploration in the new environment, mice were presented with two 30-s, 4.5-kHz, 75-dB tones identical to the training tone with a 30-s interval. Data for context freezing on day 2 and freezing to in response to tone were analyzed by two-way ANOVA with line (F-S/F-R) and sex as between-subject factors.

Fear conditioning

Naïve selected generation 4 (S4) males and 8–12-week-old females from 14 F-R and 11 F-S breeding pairs were used for these experiments. One hundred and twenty-seven male and female mice were fear conditioned with one of three training conditions, all of which utilized a 30-s, 5-kHZ, 75-dB pure tone auditory CS: (i) two presentations of the CS co-terminating in a 2-s, 0.5-mA foot shock (2 × 0.5), with a 30-s interval; (ii) two presentations of the CS co-terminating in a 2-s, 1-mA foot shock with a 30-s interval (2 × 1.0); or (iii) 10 CS presentations co-terminating in a 2-s, 0.5-mA foot shock with a variable inter-trial interval (10 × 0.5). Data for two 2 × 1.0 mice were lost because of camera failure, and seven mice in the 2 × 0.5 and 2 × 1.0 training groups had freezing levels outside two standard deviations from the mean, and were dropped from analysis as outliers. Because the determination of cued fear was based on an auditory stimulus, and early-onset deafness is sometimes found in the DBA/2 parent strain (Zheng *et al.*, 1999), videos from F-S and F-R mice with <10% freezing in response to tone 1 of the cued memory test were reviewed for an orienting response. We wanted to exclude the possibility that the cued fear response in either group, but primarily F-R mice, was artificially reduced because of hearing impairment. In two sibling mice, it could not be determined whether the mouse heard the tone (i.e. pausing briefly or turning towards the sound). These two mice were among the seven mice excluded.

One day after training, cued fear memory was tested in the alternative context (described above), with two 30-s 5-kHz, 75-dB tones with a 30-s interval. Final numbers for each experiment are stated in the figure legends. Freezing was scored using FREEZEFRAME (Coulbourn Instruments, Whitehall, PA, USA). Freezing in the training context and novel

test context prior to the first tone CS (pre-training and pre-testing baseline freezing) and freezing in response to each CS during training and testing were determined. Mean freezing in response to the two test CSs is presented.

Sample collection for enzyme-linked immunosorbent assay (ELISA)

Urine samples were collected between 07:30 h and 08:30 h from naïve male offspring of five F-S and six F-R breeding pairs (seven F-S and eight F-R). Mice were 8–11 weeks old (mean age: F-S, 10 weeks; F-R, 8.25 weeks). Collection was performed over three consecutive days. Samples were diluted 1 : 10 in the dilution buffer provided with the ELISA kit, and stored at −20 °C.

Corticosterone ELISA

Corticosterone concentrations were determined with an AssayMax corticosterone ELISA kit (AssayPro, St Charles, MO, USA). Absorbance of standards and samples was read on a Tecan microplate reader (Tecan, Research Triangle Park, NC, USA). Samples were run in triplicate, and concentrations were calculated from mean absorbance. Corticosterone concentrations in urine samples were determined from a six-point standard curve. Corticosterone concentrations were quantified in 13 samples from seven F-S males and 14 samples from eight F-R males. For mice with replicate samples, corticosterone concentrations for the 2 days were averaged and plotted as a single data point.

Quantitative polymerase chain reaction (qPCR)

A separate cohort of naïve adult S3 and S4 F-S and F-R mice was used (30 F-S and 51 F-R). The hypothalamus was rapidly dissected from 1.5-mm coronal sections with a 16-gauge needle, and immediately frozen in dry ice. Total RNA was extracted from homogenized tissue with the RNeasy Minikit (Qiagen, Valencia, CA, USA). Oligonucleotide primers were designed with PRIMER 3 software for the genes for corticotrophin-releasing hormone (CRH), CRH receptor 1 (CRHR1), mineralocorticoid receptor (MR), and glucocorticoid receptor (GR), and two reference genes: the β-actin gene and the β_2-microglobulin gene. Reactions were quantified with the cycle threshold method with SDS 2.2 software (Applied Biosystems). An average quantity value (Qty mean) for each sample, run in duplicate, was calculated for each gene. The geometric mean of the Qty mean of the β_2-microglobulin and β-actin genes was calculated. The data for each gene were expressed as Qty mean for the gene of interest/geometric mean of Qty mean for the two reference genes.

MEMRI

MEMRI was conducted on male F-S ($n = 7$) and F-R ($n = 7$) age-matched and weight-matched S4 mice. Mice ($n = 14$) were treated with Mn^{2+} in 400 mM bicine buffer (pH 7.4) continuously over 3 days with a micro-osmotic pump (1.0 μL/h; Model 1003D; Alzet, Durect Corp., Cupertino, CA, USA), giving a cumulative final $MnCl_2$ dose of 180 mg/kg ($MnCl_2.4H_2O$; Sigma-Aldrich). This Mn^{2+} dose produces significantly enhanced T1-weighted magnetic resonance imaging (MRI) signal intensity without observable toxicity (Mok *et al.*, 2011). Mice (two F-R) not implanted with a micro-pump were scanned to estimate the relative change in T1-weighted MEMRI signal intensity (SI). Mice underwent

fear conditioning at the end of Mn^{2+} dosing (day 3; data not shown). We interpreted the functional MEMRI results as representing basal activity, because Mn^{2+} uptake in the brain was slow and occurred over 72 h in the home cage prior to conditioning.

MEMRI acquisition

MRI was conducted at the end of day 3 with a 7-T Bruker BioSpec imaging system (Bruker Biospin, Billerica, MA, USA) with a 20-cm horizontal inner bore diameter and a dedicated mouse phased-array ($n = 4$) head coil. Images were acquired in anesthetized mice (1.5–2% isoflurane), by use of a three-dimensional (3D) rapid acquisition with refocused echoes sequence: repetition time, 200 ms; echo time, 6.81 ms; rapid acquisition with refocused echoes factor, 2; image matrix, 192 × 168 × 128; isotropic resolution, 100 μm. The total scan time was 72 min. During scanning, mice were monitored for temperature, respiration, and heart rate.

MEMRI functional analysis

The influence of surface coil location on SI for MEMRI images was reduced with the inhomogeneity N3 correction (Sled *et al.*, 1998) (MIPAV; NIH, Bethesda, MD, USA). Mean SI was measured from several regions of interest (ROIs). ROI alignment was conducted by an experimenter blinded to mouse phenotype. A predefined mouse atlas was used to delineate 14 3D ROIs (VIVOQUANT; InviCRO, Boston, MA, USA). We manually segmented eight additional 3D ROIs (VIVOQUANT) to incorporate a fear memory circuit into the analysis (Maren & Quirk, 2004; Pape & Pare, 2010). Manual 3D ROIs were the dorsal hippocampus, ventral hippocampus, lateral amygdala (LA), basal amygdala, central amygdala, prelimbic cortex, infralimbic cortex, and periaqueductal gray. Finally, we designated seven additional two-dimensional ROIs within the hippocampus, sampling from one rostral and one caudal location. We anatomically segregated subfields of the dorsal (CA1, CA3, and dentate gyrus) and ventral (CA1, CA2, CA3, and dentate gyrus) hippocampus, because of the high T1-weighted contrast in these areas (Fig. 5). All 3D ROIs were bilateral, and all 2D ROIs were unilateral (right ventral hippocampus and left dorsal hippocampus). Manually defined ROIs were delineated according to anatomical reference points and a stereotaxic mouse atlas (Franklin & Paxinos, 2008). For functional comparisons, each ROI was normalized by use of the whole brain SI. In the first step of the normalization procedure, the SI of the whole brain was calculated for each subject by using a mean of the 14 predefined 3D ROIs (described above). Next, the whole brain SI for each subject was normalized to the mean whole brain SI of the group. In the final step, the ROI SI for each subject was divided by its own normalized mean whole brain SI. Relative Mn^{2+} enhancement was determined by calculating the percentage change in SI for each ROI from the corresponding ROI SI of the group without Mn^{2+}. Additional measurements were conducted to validate the quality of whole brain normalization procedure described above (Supporting information). Percentage change in SI was the dependent variable in data reduction [principal components analysis (PCA)].

MEMRI volumetric analysis

Lines were established by use of a hippocampus-dependent behavioral task (contextual fear conditioning). Therefore, we hypothesized that structural alterations related to the phenotype would most likely be located in the hippocampus. The hippocampus was reconstructed in

three dimensions from N3-corrected raw MEMRI scans (VIVOQUANT). Volume (mm^3) was the dependent variable for statistical analyses.

Statistical analysis

Fear conditioning was analyzed with ANOVA, with line (F-S/F-R), sex and training (2 × 0.5, 2 × 1.0, and 10 × 0.5) as between-subject variables, and day (training/test) and segment (pre-CS baseline, CS1, and CS2) as within-subject variables. Subsequent baseline-subtracted conditioned freezing was compared by use of three-way repeated measures ANOVA, with day as the within-subject variable and line, sex and training as between-subject variables (baseline subtraction detailed below). qPCR data were compared by use of two-way ANOVA, with line and sex as between-subject variables. For ANOVA, interactions were reported first. Where there were no interactions, main effects were reported. Follow-up analyses were conducted with one-way ANOVA, with Bonferroni correction for multiple comparisons or independent samples *t*-tests for single comparisons. Corticosterone concentrations were compared between lines by use of independent samples *t*-tests.

PCA

PCA was used to visualize and interpret brain-wide activity patterns. PCA is a data reduction technique used to capture hidden patterns that best explain variance in large datasets. Here, PCA was used to visualize functional brain circuits. The result of PCA is a set of loadings and scores. Loadings are typically used to visualize and interpret patterns. PCA was used in this study not to visualize patterns as such, but rather to extract patterns that reflect underlying phenotypic differences in basal brain-wide network cellular activity. To this end, scores were used to determine which, if any, of the principal components (PCs) could account for a pattern of brain activity associated with the phenotype. Component scores provide an index of where individuals are distributed along a particular component. We grouped scores by phenotype to evaluate differences in the pattern of brain activity associated with each component. The variables for PCA were the mean ROI SIs. All variables were log-transformed prior to PCA. A covariance matrix PCA was chosen to generate a more defined component structure. Loadings were subject to varimax rotation to maximize simplicity, interpretation and orthogonality among components. Unless otherwise noted, all statistical comparisons between phenotype were conducted with one-way ANOVA. Correlations were conducted with Pearson's *r*. Statistical analyses were conducted with SPSS (IBM SPSS, Armonk, New York, USA) and GRAPHPAD PRISM (GraphPad Software, La Jolla, CA, USA). Values in the text represent the mean ± standard error of the mean. Statistical significance was set at <0.05 for all comparisons.

Results

Behavioral phenotyping

In S2, there was a sex × line interaction ($F_{1,55} = 45.57$; $P < 0.0001$) in the contextual fear test. F-S males froze more than F-S females ($P < 0.0001$) and F-R mice of either sex ($P < 0.0001$) (Fig. 1B). F-S females froze more than F-R mice ($P < 0.0001$) (Fig. 1B). In the cued fear test, there was a main effect of line ($F_{1,52} = 13.34$; $P = 0.0006$). No other effects or interactions of sex were identified in either S1 or S3, and may be stochastic. Main effects of

line were identified in context ($F_{1,54}$ = 244.72; P < 0.0001) and cued ($F_{1,53}$ = 16.08; P = 0.0002) fear tests in the S3 breeding population (Fig. 1C). These results indicate that the behavioral spectrum of the AIL population was broad, as would be expected in a natural population. Selecting from the extreme tails of the spectrum in this way established a robust phenotype in S4.

Behavioral responding in F-R and F-S lines

Differences between the F-S and F-R lines in acquisition and cued fear were evaluated in S4. Differences between F-S and F-R mice were detectable both between and within training and test days. ANOVA identified line × day ($F_{1,105}$ = 17.61; P < 0.0001) and line × segment ($F_{2,210}$ = 6.579; P = 0.002) interactions, indicating that, as expected, behavioral differences were detectable both between days and within test or training days. During training, there was a line × segment interaction ($F_{1,115}$ = 15.707; P < 0.0001). There was a small but significant difference in freezing between F-S (9.3%) and F-R (5.2%) mice during the first tone, before the shock was applied (P = 0.0003), which may reflect an orienting response or a low level of anxiety, but does not reflect fear, as the first shock was not presented until the end of the tone. At CS2, F-S mice still froze more than F-R mice (F-S, 35.7%; F-R, 21.17%; P < 0.0001) (Fig. 2).

On day 2 (test), F-S mice always froze more than F-R mice ($F_{1,115}$ = 40.472; P < 0.0001) (Fig. 2B, D, and F). Phenotypic differences in cued fear were not disrupted by increasing training intensity (2 × 1.0) or duration (10 × 0.5). However, the more intensely trained F-R mice showed similar (main effect of day: F-S 2 × 0.5 as compared with F-R 2 × 1.0, $F_{1,39}$ = 38.29, P < 0.0001) or even greater (segment × day interaction: F-R 2 × 0.5 as compared with F-R 10 × 0.5, $F_{1,33}$ = 26.47, P < 0.0001; train, P = 0.006; test, P = 0.0009) levels of freezing on day 1 (training) than F-S mice subjected to the milder 2 × 0.5 training paradigm on day 1 (Fig. 2G and H). However, in spite of the difference in fear load at acquisition, F-S mice froze more than F-R mice when tested for fear memory expression 24 h later, implicating a genetically determined difference in fear memory stabilization and consolidation (Fig. 2G and H).

Two-way ANOVA of day and line on pre-tone baseline freezing identified an interaction ($F_{1,105}$ = 18.285; P < 0.0001). Before training, baseline freezing in a novel environment was identical between F-S and F-R mice (P = 0.58) (Fig. 3A). However, after training, F-S mice showed a pronounced freezing response to a novel context (testing chamber) (P < 0.0001) (Fig. 3B). Initial differences in pre-cue freezing on day 2 between F-S and F-R mice complicate the interpretation of the cued fear response. Differences in baseline fear were addressed by subtracting baseline freezing from cued freezing within subjects (Fig. 3). We hypothesized that baseline freezing on day 2 would disproportionally affect CS1 freezing. When baseline was subtracted from CS1, a line × sex interaction emerged ($F_{1,105}$ = 5.47; P = 0.021). Cued freezing in response to tone 1 remained statistically significant in males (P = 0.001) (Fig. 3C) but not in females (P = 0.88) (Fig. 3D). Fear generalization at baseline in F-S and F-R females was identical to that in their male counterparts. Potentially, the interactions between generalized fear and cued fear differ in males and females. Further

study is required to allow firm conclusions to be drawn regarding sex differences in cued fear in F-S and F-R mice.

Regulation of the HPA axis

Morning secreted corticosterone differed between F-S and F-R mice (F-S > F-R; $P = 0.004$) (Fig. 4A). CRH mRNA expression was higher in F-S mice than in F-R mice ($P = 0.029$) (Fig. 4B), whereas expression levels of both MR and CRHR1 were lower ($P < 0.001$ for each) in F-S mice than in F-R mice (Fig. 4C and D). There was no significant difference in GR expression between F-S mice and F-R mice ($P = 0.08$; Fig. 4E). The level of GR expression relative to the level of MR expression may be particularly important, given the distinct roles of the two corticosteroid receptors.

MEMRI

MEMRI was used to study the brain structure and function of F-S and F-S mice *in vivo*. Activity across a wide range of brain regions was measured, including regions associated with fear and stress. PCA was applied to the dataset to help in the visualization and interpretation of patterns of brain activity. To account for outliers, we omitted cases with PCA scores for PC1 that were ±1.5 times the interquartile range (one F-S and one F-R), and re-ran the PCA ($n = 12$). PCA was conducted on 12 cases and 29 brain regions, resulting in seven PCs. A statistical comparison (one-way ANOVA) of the scores for each PC (1–7) indicated that only PC3 segregated the phenotype ($F_{1,10} = 23.1$; $P = 0.001$). None of the remaining PCs (1–2 and 4–7) reached statistical significance (Table 1). These results indicate that the covariance associated with PC3 represents a unique pattern of activity that is directly related to the phenotype. We interpret the remaining PCs (1–2 and 4–7) as reflecting sources of variance unrelated to the phenotype, such as population heterogeneity of the AIL, lingering inhomogeneity in the MEMRI signal (including, perhaps, minor differences in positioning within the head coil), or non-specific uncontrollable events such as occur in a shared housing facility. Loadings associated with PC3 were examined to interpret the structure of the extracted pattern. Loadings represent the substantive importance of a given variable (ROI) to the component. Examination of the rotated component matrix indicated that the amygdala and hippocampus loaded on PC3, suggesting that neuronal activity in these areas cluster together and relate to one another (Table 1). In particular, the LA, CA2, dorsal hippocampus, dorsal CA1, ventral CA1 and ventral CA3 loaded on PC3. Reconstruction of the hippocampus from MEMRI-enhanced images identified no volumetric differences between F-S and F-R mice (Fig. 5).

Discussion

Using bi-directional selection, we generated mouse lines with high (F-S) or low (F-R) fear expression after fear conditioning. First, we explored whether acquisition defects explained the differences between F-S and F-R mice in conditioned fear memory. Importantly, freezing in F-R mice increases with increased training intensity, indicating that the fear memory deficit is probably not caused by deficient learning but is a true fear memory phenotype. Whereas F-R mice could achieve equivalent or even greater levels of freezing during acquisition (day 1), F-R mice froze less on day 2 when the cue was presented (Fig. 2),

implicating memory stabilization and consolidation processes. Before fear conditioning, freezing in a novel context was equivalent between lines (Fig. 3). After fear conditioning, however, F-S mice showed greater fear in a novel environment, suggesting either greater fear generalization or threat appraisal in F-S mice (Dunsmoor *et al.*, 2009; Britton *et al.*, 2011). Glucocorticoid signaling clearly impacts on fear memory formation (Thompson *et al.*, 2004; Rodrigues *et al.*, 2009); however, whether genetic selection for fear memory established intrinsic HPA axis differences was unknown. Morning corticosterone levels were higher in F-S mice, and hypothalamic CRH, CRHR1 and MR mRNA expression differed between F-S and F-R mice (Fig. 4). These results support the behavioral phenotypes, as corticosterone strengthens contextual fear memory (Thompson *et al.*, 2004) and increases fear generalization (Kaouane *et al.*, 2012). Furthermore, both the CRH system and corticosteroid receptors are implicated in psychopathology related to fearfulness, hyper-arousal, and anxiety (de Kloet *et al.*, 1998; Gold & Chrousos, 2002; Derijk *et al.*, 2011). Finally, we identified functional differences within the limbic fear network by using *in vivo* MEMRI (Drapeau & Nachshen, 1984; Silva *et al.*, 2004). Neural activity in the LA and hippocampus was enhanced in F-S mice as compared with F-R mice (Fig. 5). These findings also align with the behavioral phenotype, as the amygdala and hippocampus are critical components of the neural circuitry underlying associative fear memory (Fig. 5) (Johnson *et al.*, 2012).

The present results extend those of previous studies using short-term selection of fear behavior (Ponder *et al.*, 2007), in several ways. Starting from an AIL rather than the F_2 cross means that smaller regions around the selected alleles were influenced by selection. Applying selective pressure to the AIL population changes the frequency of trait-relevant alleles without having a systematic impact on trait-irrelevant alleles, and we can be more confident that correlations are attributable to the selected alleles. Additionally, in an AIL, the frequency of all alleles should be ~0.5, which is optimal for bi-directional selection. Whereas the previous study identified mRNAs that were differentially expressed between high-fear and low-fear mice after fear conditioning, here we examined divergent traits in F-S and F-R mice. Our strategy of short-term, rather than longer-term, selection is advantageous because the frequency of trait-relevant alleles is changed with minimal random genetic drift (Belknap *et al.*, 1997). Generating an AIL for short-term selective breeding is a superior approach, because it increases the likelihood that observed differences between the selected lines result from selection rather than drift of linkage between selected and non-selected alleles. We selected fear phenotypes based on freezing, a validated and quantifiable measure of fear behavior in rodents (Blanchard & Blanchard, 1969b; a; Fanselow, 1980). Pain sensitivity and baseline differences in locomotion potentially influence the degree of freezing after fear conditioning. Previous work in the F_2 intercross of the C57BL/6 and DBA/2 strains found no differences in shock sensitivity or locomotor activity (Ponder *et al.*, 2007), so the behavioral phenotypes most likely relate directly to the anatomical, physiological and molecular mechanisms of fear acquisition and memory (Fig. 6).

The mechanisms and circuitry of fear memory consolidation established in rodent models translate directly to the study of humans and pathological fear (Johnson & Ledoux, 2004; Delgado *et al.*, 2006). Stronger conditioned associations and generalization of fear to non-threatening stimuli are reported in PTSD (Orr *et al.*, 2000; Peri *et al.*, 2000), anxiety disorders (Lissek *et al.*, 2005; Lissek *et al.*, 2010), and depression (Nissen *et al.*, 2010). More

importantly, prospective studies in first-responders demonstrate that 'conditionability' predicts the psychological impact of later trauma (Guthrie & Bryant, 2006; Orr *et al.*, 2012). F-S and F-R lines therefore provide a translational tool for identifying underlying determinants of fear memory strength as well as susceptibility and resistance to fear-related psychopathology.

Alterations in circadian corticosteroid rhythms are proposed endophenotypes of anxiety disorders, affective disorders, and PTSD (Baker *et al.*, 2005; Wichers *et al.*, 2008; Lok *et al.*, 2012). In non-human primates, cortisol levels correlate with defensive freezing (Kalin *et al.*, 1998), whereas in humans, higher basal cortisol levels are positively correlated with fear learning (Pineles *et al.*, 2012), fear anticipation, amygdala activation (Grillon *et al.*, 2006; Merz *et al.*, 2012), and fear-potentiated startle (Grillon *et al.*, 2006). In human populations, the relationship between HPA axis regulation and psychopathology is not always as straightforward (Klaassens *et al.*, 2012; Lok *et al.*, 2012); however, F-S and F-R lines may provide a tool for identifying traits that could prospectively identify at-risk individuals (Lok *et al.*, 2012).

Basal cortisol levels may directly impact on neural fear networks. Resting prefrontal–amygdala connectivity inversely relates to basal cortisol levels (Veer *et al.*, 2012), and alterations in the resting-state connectivity of the fear and emotion circuitry have been reported in pathological anxiety (Indovina *et al.*, 2011), depression (Veer *et al.*, 2010), and PTSD (Sripada *et al.*, 2012). Using MEMRI, we uncovered differences between F-S and F-R lines in a well-characterized amygdala–hippocampus circuit (LeDoux, 2000; Rodrigues *et al.*, 2009). One caveat to our interpretation is that all mice underwent fear conditioning at the end of $MnCl_2$ dosing. We interpreted our results as representing basal activity, because the Mn^{2+} infusion dose rate was low (1.0 μL/h) and continuous over a period of 72 h before conditioning. Slow infusion of Mn^{2+} over a period of 72 h reduces the Mn^{2+} concentration gradient at any one point in time (Mok *et al.*, 2011). Therefore, residual Mn^{2+} in the extracellular space after infusion was effectively negligible, and not likely to contribute significantly to the final distribution pattern of Mn^{2+}. Mn^{2+} enters cells through multiple Ca^{2+} transporter proteins (Drapeau & Nachshen, 1984; Hankir *et al.*, 2012), including those implicated in fear learning-induced neuroplasticity (Rodrigues *et al.*, 2004; Johansen *et al.*, 2011). Therefore, MEMRI indicated more Ca^{2+}-dependent activity in the fear learning circuit of F-S mice. Enhanced activity in F-S mice was predominantly localized to the hippocampus (Fig, 5). This finding is significant because of hippocampal involvement in contextual fear conditioning (Lee & Kesner, 2004; Daumas *et al.*, 2005). There were no corresponding increases in hippocampal volume (Fig. 5), suggesting that functional differences in the hippocampus are independent of structural differences.

Differential expression of HPA axis regulatory genes probably contributes to F-S and F-R memory phenotypes. MR, but not GR, is downregulated in F-S mice relative to F-R mice. MR is primarily expressed in the hypothalamus and hippocampus, and exerts tonic control of the HPA axis through high-affinity binding of glucocorticoids (Kovacs & Mezey, 1987; Han *et al.*, 2005). Importantly, MR is also an important contributor to fear memory formation (Zhou *et al.*, 2010). Inhibition of MR signaling (Ratka *et al.*, 1989; Berger *et al.*, 2006; Brinks *et al.*, 2009) enhances fear learning and generalization, and alters circadian

corticosterone levels. Expression of GR is equivalent between F-S and F-R mice. F-S and F-R mice may therefore differ in MR/GR ratio. The relative contributions of MR–GR signaling impacts on aspects of cognition and behavior in rodents (Harris *et al.*, 2012), and may contribute to affective disorders in humans (de Kloet *et al.*, 1998; Qi *et al.*, 2012).

Genes regulating the HPA axis play a role in psychopathology independently of corticosteroids. Upregulation of CRH may contribute to the elevated basal corticosterone levels found in F-S mice. However, brain CRH levels are also associated with fear and anxiety (Kalin & Takahashi, 1990), PTSD (Baker *et al.*, 1999), and depression (Nemeroff *et al.*, 1984; Wang *et al.*, 2009). Conversely, mRNA for CRHR1 is decreased in F-S mice. Evidence from CRHR1 knockout mice suggests that hypothalamic CRHR1 signaling negatively regulates basal corticosterone prior to weaning (Schmidt *et al.*, 2006), but whether this inhibitory regulation is maintained into adulthood is not clear. Alternatively, CRHR1 downregulation may be compensatory in the response to increased corticosteroid signaling (Nemeroff *et al.*, 1988). However, CRHR1 polymorphisms and reduced CRHR1 binding are associated with psychopathology (Nemeroff *et al.*, 1988; Gillespie *et al.*, 2009; Wasserman *et al.*, 2010). How CRHR1 downregulation in the hypothalamus relates to the fear memory phenotype of F-S and F-R mice is unknown, but it represents a marker for future study (Fig. 6).

Rapid selection in AILs for fear phenotypes provides a unique opportunity to isolate a coordinated network of traits establishing fear susceptibility and resistance. Recent studies have identified an increased ‘fear load’ in PTSD patients, suggesting that people with PTSD have an exaggerated memory for and poor discrimination of fearful vs. neutral cues (Felmingham *et al.*, 2003; Jovanovic *et al.*, 2012). In F-S mice, we identified similar behavioral differences corresponding to pre-existing differences in HPA axis regulation and limbic circuit activity between F-S and F-R lines.

Prospective studies of fear pathology in human populations are difficult to implement and interpret, expensive, and therefore infrequent. However, the identification of traits and systems predisposing individuals to strongly encode fear memory is important for developing targeted, efficacious interventions for PTSD and other fear-related disorders. The identification of fear-resistance factors may identify additional treatment strategies. Bi-modal selection from an AIL facilitates enquiry along each of these lines. These studies in naive animals have established that F-S and F-R mouse lines have robust differences in fear learning and memory and distinct physiological traits.

Supplementary Material

Refer to Web version on PubMed Central for supplementary material.

Acknowledgments

We would like to thank Dr Laura Tucker, Dr Asamoah Bosomti, Ann Schue, Sumajari Das, Smita Dey, Maj Robert Long, Rose Arditi and Alice Fladung for excellent assistance with aspects of this project. This project was funded by CSTS grant G188NW to L. R. Johnson, by NIH R01MH079103 to A. A. Palmer, and by T32DA007255 to C. C. Parker.

Abbreviations

AIL	advanced intercross line
CRH	corticotrophin-releasing hormone
CRHR1	corticotrophin-releasing hormone receptor 1
CS	conditioned stimulus
3D	three-dimensional
ELISA	enzyme-linked immunosorbent assay
F-R	fear-resistant
F-S	fear-susceptible
GR	glucocorticoid receptor
HPA	hypothalamic–pituitary–adrenal
LA	lateral amygdala
MEMRI	manganese-enhanced magnetic resonance imaging
MR	mineralocorticoid receptor
MRI	magnetic resonance imaging
PC	principal component
PCA	principal components analysis
PTSD	post-traumatic stress disorder
qPCR	quantitative polymerase chain reaction
ROI	region of interest
S1	selected generation 1
S2	selected generation 2
S3	selected generation 3
S4	selected generation 4
SI	signal intensity
USUHS	Uniformed Services University of the Health Sciences

References

Amstadter A, Nugent N, Koenen K. Genetics of PTSD: fear conditioning as a model for future research. Psychiatr. Ann. 2009; 39:358–367. [PubMed: 19779593]

Baker D, Ekhator N, Kaskow J, Dashevsky B, Horn P, Bedarnik L, Geracioti T. Higher basal serial CSF cortisol in combat veterans with posttraumatic stress disorder. Am. J. Psychiatry. 2005; 162:992–994. [PubMed: 15863803]

Baker D, West S, Nicholson W, Ekhator N, Kaskow J, Hill K, Bruce A, Orth D, TD G. Serial CSF corticotropin-releasing hormone levels and adrenocortical activity in combat veterans with posttraumatic stress disorder. Am. J. Psychiatry. 1999; 156:585–588. [PubMed: 10200738]

Belknap J, Richards S, O'Toole L, Helms M, Phillips T. Short-term selective breeding as a tool for QTL mapping: ethanol preference drinking in mice. Behav. Genet. 1997; 27:55–65. [PubMed: 9145544]

Berger S, Wolfer DP, Selbach O, H A, Erdmann G, Reichardt HM, Cheplova AN, Welzl H, Haas HL, Lipp H-P, Schutz G. Loss of the limbic mineralocorticoid receptor impairs behavioral plasticity. Proc. Natl Acad. Sci. USA. 2006; 103:195–200. [PubMed: 16368758]

Blanchard RJ, Blanchard DC. Crouching as an index of fear. J. Comp. Physiol. Psychol. 1969a; 67:370–375. [PubMed: 5787388]

Blanchard RJ, Blanchard DC. Passive and active reactions to fear-eliciting stimuli. J. Comp. Physiol. Psychol. 1969b; 68:129–135. [PubMed: 5793861]

Brinks V, Berger S, Gass P, de Kloet ER, Oitzl MS. Mineralocorticoid receptors in control of emotional arousal and fear memory. Horm. Behav. 2009; 56:232–238. [PubMed: 19447109]

Britton J, Lissek S, Grillon C, Norcross B, Pine D. Development of anxiety: the role of threat appraisal and fear learning. Depression Anxiety. 2011; 28:5–17. [PubMed: 20734364]

Daumas S, Halley H, Frances B, Lassalle J. Encoding, consolidation, and retrieval of contextual memory: differential involvement of dorsal CA3 and CA1 hippocampal subregions. Learn. Mem. 2005; 4:375–383.

de Kloet E, Vreugdenhil E, Oitzl M, Joels M. Brain corticosteroid receptor balance in health and disease. Endocr. Rev. 1998; 19:269–301. [PubMed: 9626555]

Delgado M, Olsson A, Phelps E. Extending animal models of fear conditioning to humans. Biol. Psychiatry. 2006; 73:39–48.

Derijk R, de Kloet E, Zitman FG, van Leeuwen N. Mineralocorticoid receptor gene variants as determinants of HPA-axis regulation and behavior. Endocr. Dev. 2011; 20:137–148. [PubMed: 21164267]

Drapeau P, Nachshen DA. Manganese fluxes and manganese-dependent neurotransmitter release in presynaptic nerve endings isolated from rat brain. J. Physiol. 1984; 348:493–510. [PubMed: 6325673]

Dunsmoor J, Mitroff S, LaBar K. Generalization of conditioned fear along a dimension of increasing fear intensity. Learn. Mem. 2009; 16:460–469. [PubMed: 19553384]

Elzinga B, Bremner J. Are substrates of memory the final common pathway in posttraumatic stress disorder (PTSD)? J. Affect. Disord. 2002; 70:1–17. [PubMed: 12113915]

Fanselow M. Conditioned and unconditioned components of post-shock freezing. Pavlovian J. Biol. Sci. 1980; 15:177–182.

Felmingham KL, Bryant RA, Gordon E. Processing angry and neutral faces in post-traumatic stress disorder: an event-related potentials study. Neuroreport. 2003; 14:77–780. [PubMed: 12544835]

Franklin, K., Paxinos, G. The Mouse Brain in Stereotaxic Coordinates. Academic Press; New York: 2008.

Gillespie C, Phifer JE, Bradley B, Ressler KJ. Risk and resilience: genetic and environmental influences on development of the stress response. Depression Anxiety. 2009; 26:984–992. [PubMed: 19750552]

Gold P, Chrousos G. Organization of the stress system and its dysregulation in melancholic and atypical depression: high vs low CRH/NE states. Mol. Psychiatry. 2002; 7:254–275. [PubMed: 11920153]

Grillon C, Pine D, Baas J, Lawley M, Ellis V, Charney D. Cortisol and DHEA-S are associated with startle potentiation during aversive conditioning in humans. Psychopharmacology. 2006; 186:434–441. [PubMed: 16052364]

Guthrie R, Bryant R. Extinction learning before trauma and subsequent posttraumatic stress. Psychosom. Med. 2006; 68:307–311. [PubMed: 16554398]

Hall C. The inheritance of emotionality. Sigma Xi Q. 1938; 26:17–28.

Han F, Ozawa H, Matsuda K, Kawata M. Colocalization of mineralocorticoid receptor and glucocorticoid receptor in the hippocampus and hypothalamus. Neurosci. Res. 2005; 51:371–381. [PubMed: 15740800]

Hankir MK, Parkinson JR, Bloom SR, Bell JD. The effects of glutamate receptor agonists and antagonists on mouse hypothalamic and hippocampal neuronal activity shown through manganese enhanced MRI. Neuroimage. 2012; 59:968–978. [PubMed: 21925279]

Harris A, Holmes M, de Kloet E, Chapman K, Seckl J. Mineralocorticoid and glucocorticoid receptor balance in control of HPA-axis and behaviour. Psychoneuroendocrinology. 2012; 38:648–658. [PubMed: 22980941]

Hettema J, Annas P, Neale M, Kendler K, Fredrikson M. A twin study of the genetics of fear conditioning. Arch. Gen. Psychiatry. 2003; 60:702–708. [PubMed: 12860774]

Indovina I, Robbins TW, Nunez-Elizalde AO, Dunn BD, Bishop SJ. Fear-conditioning mechanisms associated with trait vulnerability to anxiety in humans. Neuron. 2011; 69:563–571. [PubMed: 21315265]

Johansen JP, Cain CK, Ostroff LE, LeDoux JE. Molecular mechanisms of fear learning and memory. Cell. 2011; 147:509–524. [PubMed: 22036561]

Johnson L, McGuire J, Lazarus R, Palmer A. Pavlovian fear memory circuits and phenotype models of PTSD. Neuropharmacology. 2012; 62:638–646. [PubMed: 21782833]

Johnson, LR., Ledoux, JE. The anatomy of fear: microcircuits of the lateral amygdala. In: Gorman, JM., editor. Fear and Anxiety: the Benefits of Translational Research. American Psychiatric Publishing; Arlington, VA: 2004. p. 227-250.

Jovanovic T, Kazama A, Bachevalier J, Davis M. Impaired safety signal learning may be a biomarker of PTSD. Neuropharmacology. 2012; 62:695–704. [PubMed: 21377482]

Kalin N, Shelton S, Rickman M, Davidson R. Individual differences in freezing and cortisol in infant and mother rhesus monkeys. Behav. Neurosci. 1998; 112:251–255. [PubMed: 9517832]

Kalin N, Takahashi L. Fear-motivated behavior induced by prior shock experience is mediated by corticotrophin-releasing hormone systems. Brain Res. 1990; 509:80–84. [PubMed: 2155045]

Kaouane N, Porte Y, Vallee M, Brayda-Bruno L, Mons N, Calandreau L, Marighetto A, Piazza PV, Desmedt A. Glucocorticoids can induce PTSD-like memory impairments in mice. Sciencexpress. 2012:1–4.

Klaassens ER, Giltay EJ, Cuijpers P, van Veen T, Zitman FG. Adulthood trauma and HPA-axis functioning in healthy subjects and PTSD patients: a meta-analysis. Psychoneuroendocrinology. 2012; 37:317–331. [PubMed: 21802212]

Koretsky AP. New developments in magnetic resonance imaging of the brain. NeuroRx. 2004; 1:155–164. [PubMed: 15717015]

Koretsky AP. Is there a path beyond BOLD? Molecular imaging of brain function. Neuroimage. 2012; 62:1208–1215. [PubMed: 22406355]

Kovacs K, Mezey E. Dexamethasone inhibits corticotropin-releasing factor expression in the rat paraventricular nucleus. Neuroendocrinology. 1987; 46:365–368. [PubMed: 3499580]

LeDoux JE. Emotion circuits in the brain. Annu. Rev. Neurosci. 2000; 23:155–184. [PubMed: 10845062]

Lee I, Kesner R. Differential contributions of the dorsal hippocampal subregions to memory acquisition and retrieval in contextual fear conditioning. Hippocampus. 2004; 14:301–310. [PubMed: 15132429]

Lissek S, Powers A, McClure E, Phelps E, Woldehawariat G, Grillon C, Pine D. Classical fear conditioning in the anxiety disorders: a meta analysis. Behav. Res. Ther. 2005; 43:1391–1424. [PubMed: 15885654]

Lissek S, Rabin S, Heller R, Lukenbaugh D, Geraci M, Pine D, Grillon C. Overgeneralization of fear as a pathogenic marker of panic disorder. Am. J. Psychiatry. 2010; 167:47–55. [PubMed: 19917595]

Lok A, Mocking R, Ruhe H, Visser I, Koeter M, Assies J, Bockting C, Olff M, Schene A. Longitudinal hypothalamic–pituitary–adrenal axis trait and state effects in recurrent depression. Psychoneuroendocrinology. 2012; 37:892–901. [PubMed: 22094110]

Mahan A, Ressler K. Fear conditioning, synaptic plasticity and the amygdala: implications for posttraumatic stress disorder. Trends Neurosci. 2012; 35:24–35. [PubMed: 21798604]

Maren S, Quirk G. Neuronal signaling of fear and memory. Neuroscience. 2004; 5:844–852. [PubMed: 15496862]

Merz C, Stark R, Vaitl D, Tabbert K, Wolf O. Stress hormones are associated with the neuronal correlates of instructed fear conditioning. Biol. Psychiatry. 2012; 92:82–89.

Mok SI, Munasinghe JP, Scott Young W. Infusion-based manganese-enhanced MRI: a new imaging technique to visualize the mouse brain. Brain Struct. Funct. 2011; 217:107–114. [PubMed: 21597966]

Nemeroff C, Owens M, Bissette G, Andorn A, Stanley M. Reduced corticotropin releasing factor binding sites in the frontal cortex of suicide victims. Arch. Gen. Psychiatry. 1988; 45:577–589. [PubMed: 2837159]

Nemeroff C, Widerlov E, Bissette G, Walleus H, Karlsson I, Eklund K, Kilts C, Loosen P, Vale W. Elevated concentrations of CSF corticotripin-releasing factor-like immunoreactivity in depressed patients. Science. 1984; 226:1342–1345. [PubMed: 6334362]

Nissen C, Holz J, Blechert J, Feige B, Riemann D, Voderholzer U, Normann C. Learning as a model for neural plasticity in major depression. Biol. Psychiatry. 2010; 68:544–553. [PubMed: 20655508]

Norrholm SD, Jovanovic T, Olin IW, Sands LA, Karapanou I, Bradley B, Ressler KJ. Fear extinction in traumatized civilians with posttraumatic stress disorder: relation to symptom severity. Biol. Psychiatry. 2011; 69:556–563. [PubMed: 21035787]

Orr S, Lasko N, Macklin M, Pineles S, Chan Y, Pitman R. Predicting post-trauma stress symptoms from pre-trauma psychophysiologic reactivity, personality traits, and measures of psychopathology. Biol. Mood Anxiety Disord. 2012; 2:1–12. [PubMed: 22738278]

Orr S, Metzger L, Lasko N, Macklin M, Peri T, Pitman R. De novo conditioning in trauma-exposed individuals with and without posttraumatic stress disorder. J. Abnorm. Psychol. 2000; 109:290–298. [PubMed: 10895567]

Pape HC, Pare D. Plastic synaptic networks of the amygdala for the acquisition, expression, and extinction of conditioned fear. Physiol. Rev. 2010; 90:419–463. [PubMed: 20393190]

Parker C, Palmer A. Dark matter: are mice the solution to missing heretibility? Front. Genet. 2011; 2:1–7. [PubMed: 22303300]

Parker C, Sokoloff G, Cheng R, Palmer A. Genome-wide association for fear conditioning in an advanced intercross mouse line. Behav. Genet. 2012; 42:437–448. [PubMed: 22237917]

Peri T, Ben-Shakhar G, Orr S, Shalev A. Psychophysiologic assessment of aversive conditioning in posttraumatic stress disorder. Biol. Psychiatry. 2000; 47:512–519. [PubMed: 10715357]

Pineles S, Rasmusson A, Yehuda R, Lasko N, Macklin M, Pitman R, Orr S. Predicting emotional responses to potentially traumatic events from pre-exposure waking cortisol levels: a longitudinal study of police and firefighters. Anxiety Stress Coping. 2012; 26:241–253. [PubMed: 22574657]

Ponder CA, Kliethermes MR, Drew MR, Muller J, Das K, Risbrough VB, Crabbe JC, TC G, Palmer AA. Selection for contextual fear conditioning affects anxiety-like behaviors and gene expression. Genes Brain Behav. 2007; 6:736–749. [PubMed: 17309658]

Qi X-R, Kamphuis W, Wang S, Wang Q, Lucassen P, Zhou J-N, Swaab D. Aberrent stress hormone receptor balance in the human prefrontal cortex and hypothalamic paraventricular nucleus of depressed patients. Psychoneuroendocrinology. 2012; 38:863–870. [PubMed: 23137715]

Ratka A, Sutanto W, Bloemers M, de Kloet E. On the role of brain mineralocorticoid (type I) and glucocorticoid (type II) receptors in neuroendocrine regulation. Neuroendocrinology. 1989; 50:117–123. [PubMed: 2550833]

Rodrigues S, LeDoux J, Sapolsky R. The influence of stress hormones on fear circuitry. Annu. Rev. Neurosci. 2009; 32:289–313. [PubMed: 19400714]

Rodrigues SM, Farb CR, Bauer EP, LeDoux JE, Schafe GE. Pavlovian fear conditioning regulates Thr286 autophosphorylation of Ca^{2+}/calmodulin-dependent protein kinase II at lateral amygdala synapses. J. Neurosci. 2004; 24:3281–3288. [PubMed: 15056707]

Schmidt M, Deussing J, Oitzl M, Ohl F, Levine S, Wurst W, Holsboer F, Muller M, de Kloet E. Differential disinhibition of the neonatal hypothalamic–pituitary–adrenal axis in brain-specific CRH receptor 1-knockout mice. Eur. J. Neurosci. 2006; 24:2291–2298. [PubMed: 17042789]

Shin L, Handwerger K. Is posttraumatic stress disorder a stress-induced fear circuitry disorder? J. Traumatic Stress. 2009; 22:409–415.

Silva AC, Bock NA. Manganese-enhanced MRI: an exceptional tool in translational neuroimaging. Schizophr. Bull. 2008; 34:595–604. [PubMed: 18550591]

Silva AC, Lee JH, Aoki I, Koretsky AP. Manganese-enhanced magnetic resonance imaging (MEMRI): methodological and practical considerations. NMR Biomed. 2004; 17:532–543. [PubMed: 15617052]

Sled JG, Zijdenbos AP, Evans AC. A nonparametric method for automatic correction of intensity nonuniformity in MRI data. IEEE Transl. Med. Imaging. 1998; 17:87–97.

Sripada R, King A, Garfinkel S, Wang X, Sripanda C, Welsh R, I L. Altered resting-state amygdala functional connectivity in men with posttraumatic stress disorder. J. Psychiatry Neurosci. 2012; 37:241–249. [PubMed: 22313617]

Thompson B, Erickson K, Schulkin J, JB R. Corticosterone facilitates retention of contextually conditioned fear and increases CRH mRNA expression in the amygdala. Behav. Brain Res. 2004; 149:209–215. [PubMed: 15129783]

Tryon W. A bidirectional associative memory explanation of posttraumatic stress disorder. Clin. Psychol. Rev. 1999; 19:789–818. [PubMed: 10520436]

Veer I, Beckman C, van Tol M, Ferrarini L, Milles J, Veltman D, Aleman A, van Buchem MA, van der Wee N, Rombouts S. Whole brain resting-state analysis reveals decreased functional connectivity in major depression. Front. Syst. Neurosci. 2010; 4:1–10. [PubMed: 20204156]

Veer I, Oei N, Spinhoven P, van Buchem M, Elzinga B, Rombouts S. Endogenous cortisol is associated with functional connectivity between the amygdala and prefrontal cortex. Psychoneuroendocrinology. 2012; 37:1039–1047. [PubMed: 22204928]

Wang SH, de Oliveira Alvares L, Nader K. Cellular and systems mechanisms of memory strength as a constraint on auditory fear reconsolidation. Nat. Neurosci. 2009; 12:905–912. [PubMed: 19543280]

Wasserman D, Wasserman J, Sokolowski M. Genetics of HPA-axis, depression and suicidality. Eur. Psychiatry. 2010; 25:278–280. [PubMed: 20444578]

Wichers M, Myin-Germeys I, Jacobs N, Kenis G, Derom C, Vlietinck R, Delespaul P, Mengelers R, Peeters F, Nicolson N, Van Os J. Susceptibility to depression expressed as alterations in cortisol day curve: a cross-twin, cross-trait study. Psychosom. Med. 2008; 70:314–318. [PubMed: 18378863]

Zheng Q, Johnson K, Erway L. Assessment of hearing in 80 inbred strains of mice by ABR threshold analysis. Hear. Res. 1999; 130:94–107. [PubMed: 10320101]

Zhou M, Bakker E, Velzing E, Berger S, Oitzl MS, Joels M, Krugers H. Both mineralocorticoid and glucocorticoid receptors regulate emotional memory in mice. Neurobiol. Learn. Mem. 2010; 94:530–537. [PubMed: 20849967]

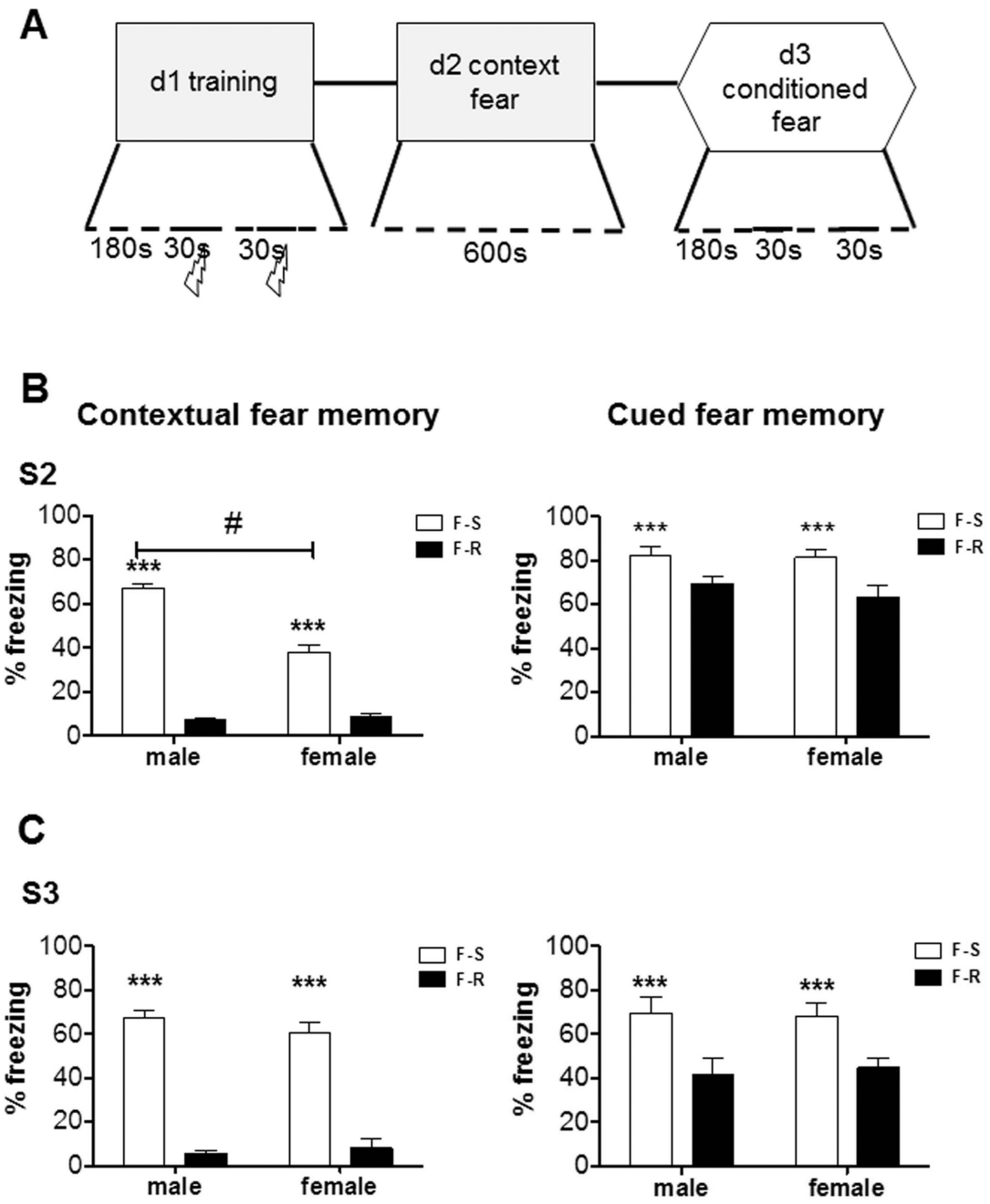

Figure 1.

(A) Diagram of fear conditioning for phenotypic selection. (B and C) Contextual and conditioned fear expression in S2 and S3 males and females selected for breeding. (B) In S2, F-S males froze significantly more than any other group, and F-S males and females froze more than F-R animals of either sex. In the cued fear test, F-S mice froze more than F-R mice. (C) In S3, there were no differences between males and females in either contextual or conditioned fear. S2 mice selected for breeding and spares: F-S males, $n = 12$; F-S females, $n = 14$; F-R males, $n = 16$; F-R females, $n = 14$. S3 mice selected for breeding and spares: F-

S males, $n = 16$; F-S females, $n = 15$; F-R males, $n = 12$; F-R females, $n = 14$. ***$P <$ 0.0001 between F-S and F-R; #$P < 0.05$ between males and females.

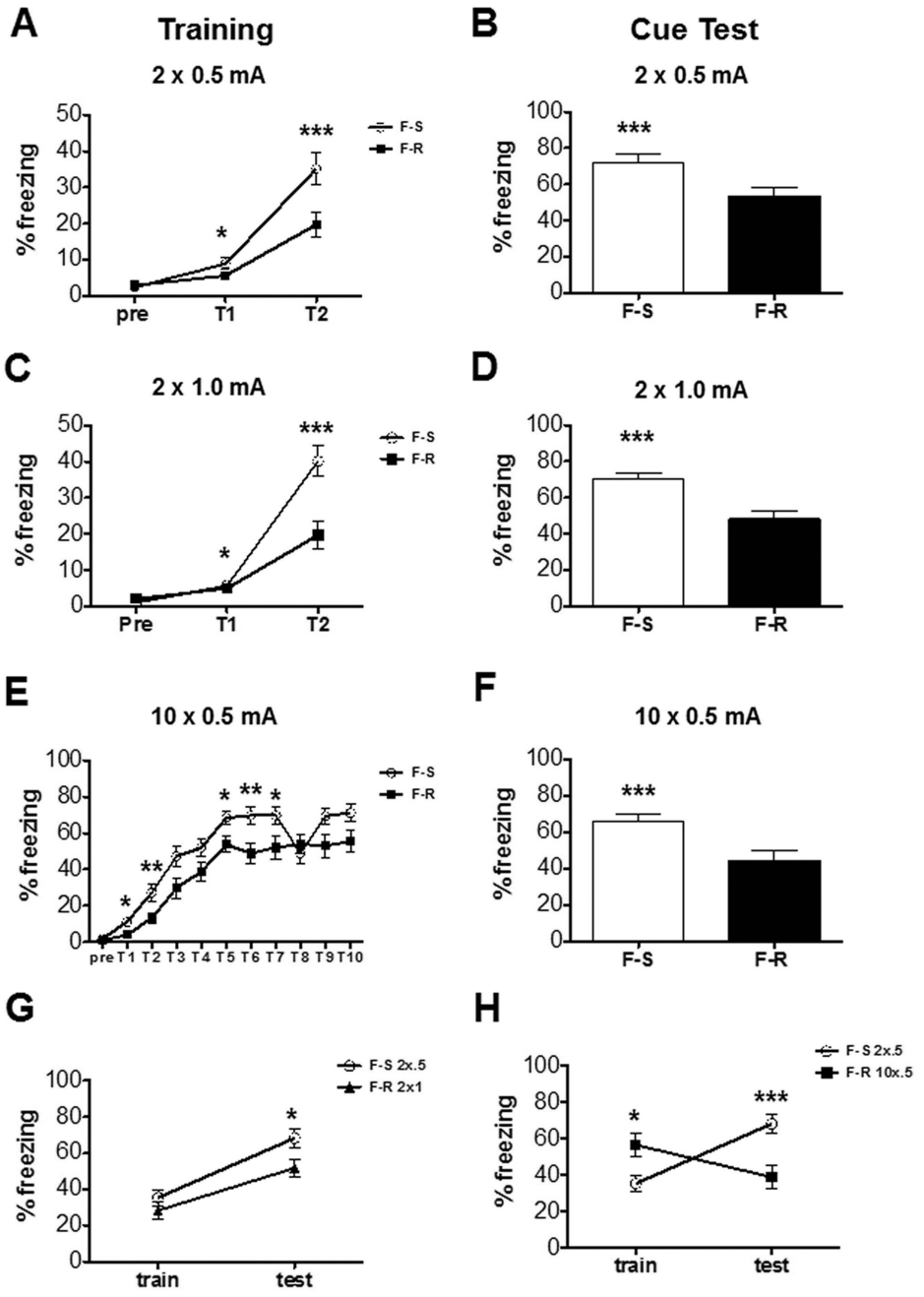

Figure 2.

F-S and F-R fear memory phenotypes are not altered by training strength. (A–F) Freezing in F-S mice was significantly higher than in F-R mice during both training. (A, C, and E) and test for cued fear (B, D, and F). (G–H) Phenotypic differences in conditioned fear depended on consolidation. F-R mice froze to the same extent (G) or more (H) at acquisition (day 1) than F-S mice when a more intense training protocol was applied, but phenotypic differences in conditioned fear memory (day 2) remained. (A–F) 2 × 0.5-mA training condition: F-S males, $n = 10$; F-R males, $n = 16$; F-S females, $n = 10$; F-R femalers, $n = 8$. 2 × 1.0-mA training condition: F-S males, $n = 7$; F-R males, $n = 11$; F-S females, $n = 15$; F-R females, n

= 9. 10 × 0.5-mA training condition: F-S males, $n = 6$; F-R males, $n = 6$; F-S females, $n = 11$; F-R females, $n = 8$. (G–H) F-S, 2 × 0.5, $n = 20$; F-R, 2 × 1.0, $n = 20$; F-R, 10 × 0.5, $n = 14$. ***$P < 0.0001$, **$P < 0.001$ and *$P < 0.05$ between F-S and F-R.

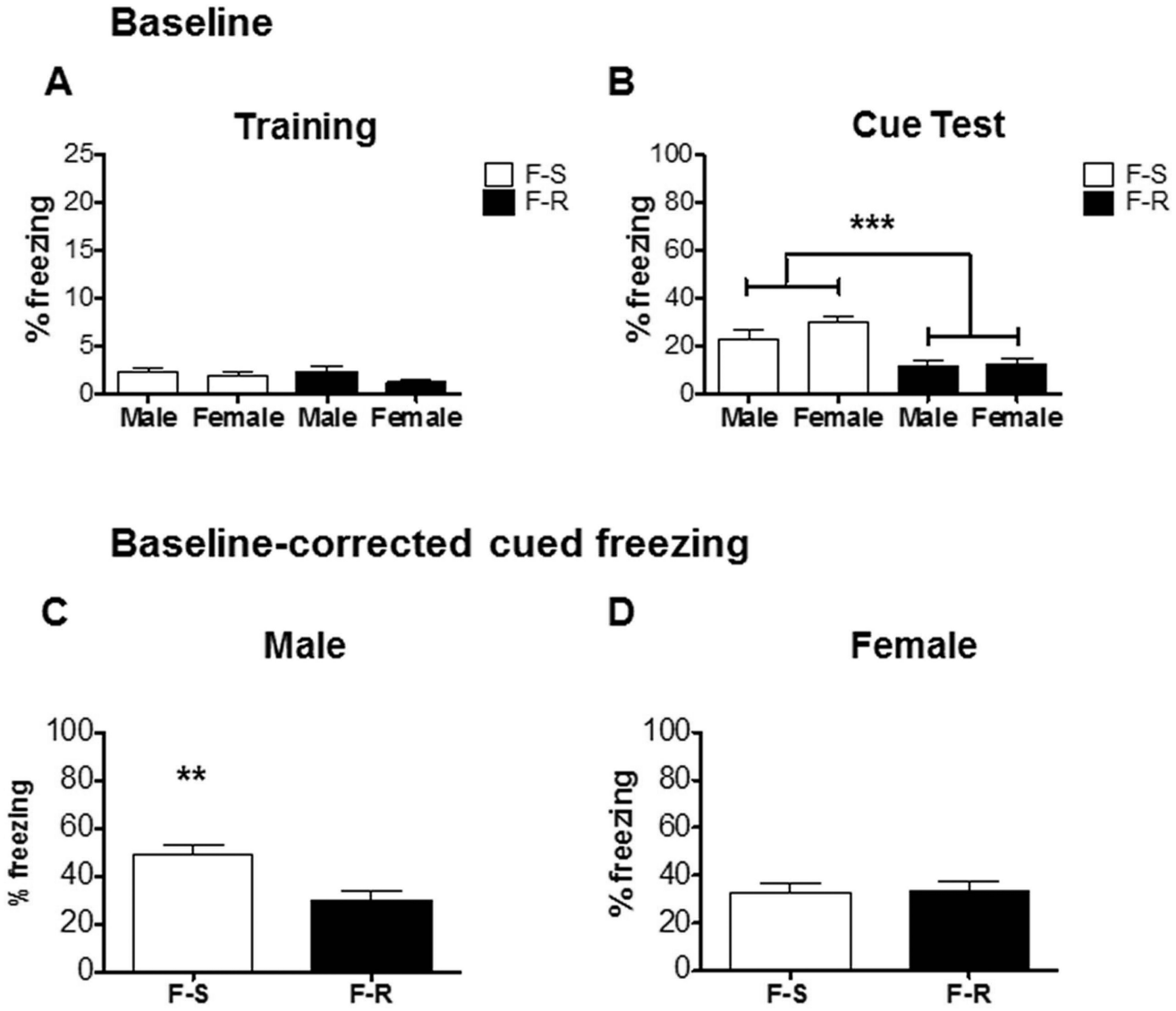

Figure 3.

F-S mice show fear generalization after conditioning. (A) Before training, there were no differences in freezing behavior in the novel training chamber. (B) After training, freezing was substantially higher in F-S mice than in F-R mice in a new (test chamber) environment. (C and D) The interaction of fear generalization was different between males and females. (C) After baseline subtraction, significant differences in the cued fear response to CS1 remained between F-S and F-R males. (D) In females, subtracting baseline freezing from the conditioned response eliminated phenotypic differences in the conditioned fear response. (A and B) F-S, $n = 59$; F-R, $n = 58$. (C and D) F-S males $n = 23$; F-R males, $n = 33$; F-S females, $n = 36$; F-R females, $n = 25$. ***$P < 0.0001$ and **$P < 0.01$ between F-S and F-R.

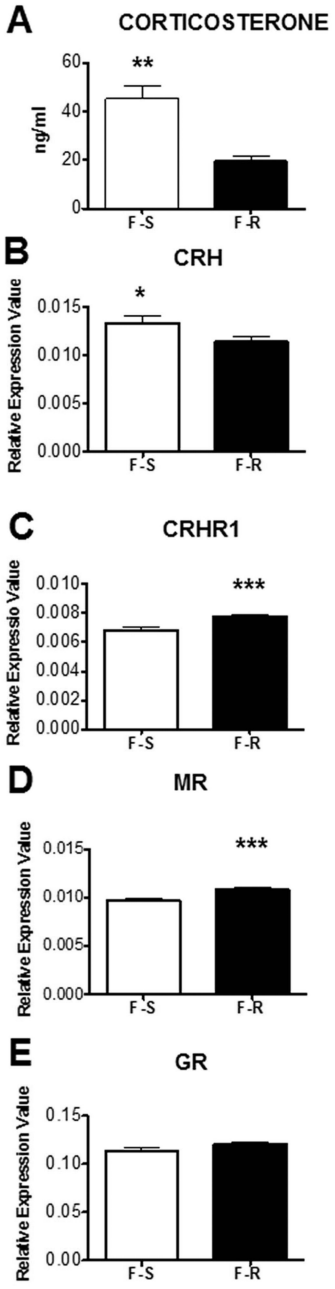

Figure 4.

F-S and F-R mice differ in basal HPA axis activity and gene expression. (A) F-S males secreted higher levels of corticosterone in urine in the circadian trough than F-R males. (B–D) qPCR analysis of relative expression of key HPA axis regulators showed an increase in CRH mRNA (B) and decreases in CRHR1 (C) and MR (D) mRNA in the hypothalamus. Data are relative expression values adjusted to β_2-microglobulin and β-actin reference genes. (A) ELISA: F-S males, $n = 7$; F-R males, $n = 8$. (B–D) qPCR: F-S males and females, $n = 30$; F-R males and females, $n = 51$. ***$P < 0.0001$, **$P < 0.01$ and *$P < 0.05$ between F-S and F-R.

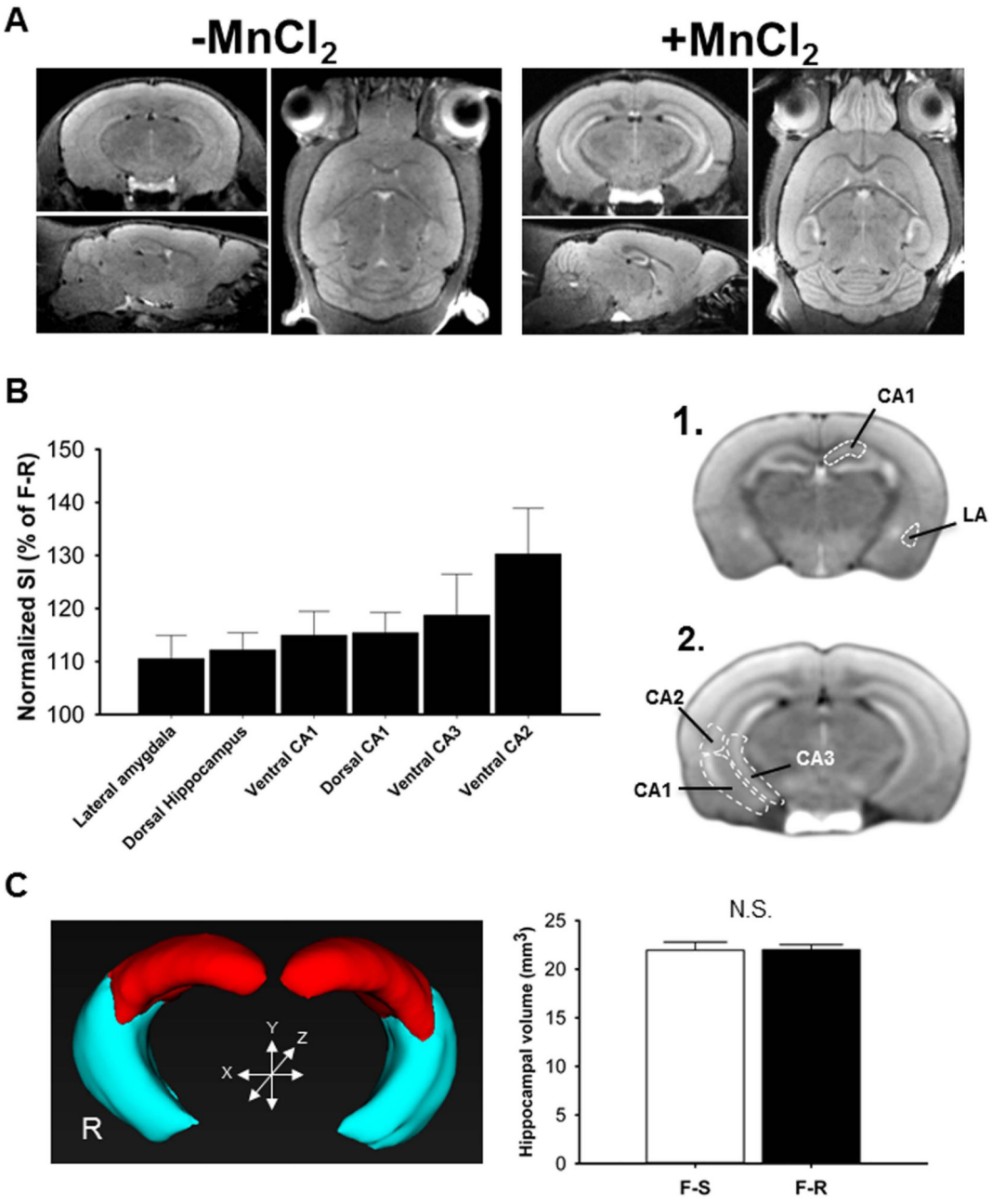

Figure 5.

MEMRI revealed that a unique and coordinated pattern of basal neuronal activity differentiates F-S and F-R mice. (A) Representative T1-weighted whole brain MRI scans (isotropic resolution, 100 μm) of a mouse brain without (−$MnCl_2$) and after (+$MnCl_2$) $MnCl_2$ infusion (180 mg/kg final dose). (B) MEMRI SI for F-S mice was normalized to F-R mice (F-S/mean F-R) for ROIs with the highest loading (>0.5) on PC3 (‘a fear memory network’). Representative MEMRI images depict ROIs that differentiated the phenotype at a (1) rostral (CA1 and LA) and (2) caudal (CA1, CA2, and C3) coronal plane. (C) Volumetric analysis of the hippocampus *in vivo*. Representative image of the mouse hippocampus

reconstructed in three dimensions from 100-μm isotropic MEMRI scans (left panel). There were no differences in hippocampal volume between lines (right panel). F-S males, $n = 6$; F-R males, $n = 6$. *$P < 0.05$ between F-S and F-R.

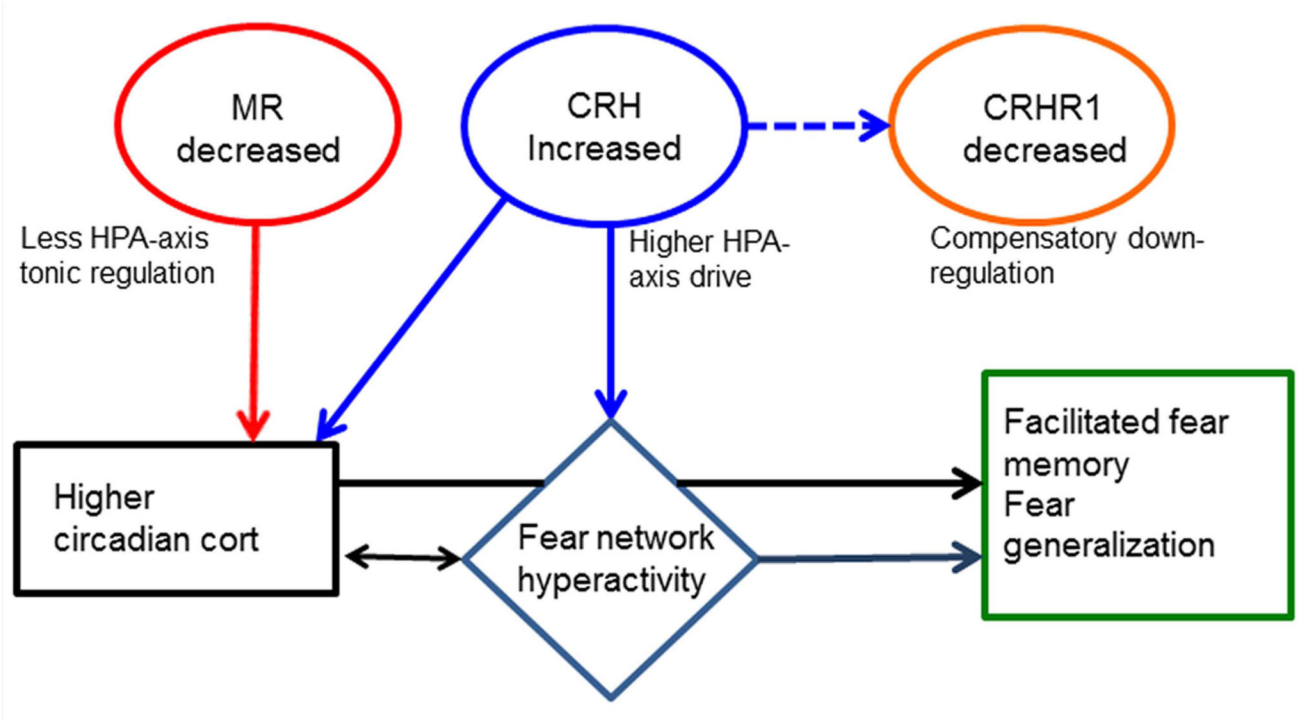

Figure 6.

Putative model of relationships between observed physical and behavioral phenotypes. Hormonal, molecular and imaging data in F-S and F-R lines suggest that these systems may independently and/or cooperatively contribute to Pavlovian fear memory phenotypes in F-S and F-R mice. cort, corticosteroid.

Table 1

Rotated component loading matrix

ROI	Component						
	1	2	3	4	5	6	7
Central amygdala	0.868						
Hypothalamus	0.831						
Basal amygdala	0.783						
Pallidum	0.763						
Prelimbic cortex	–0.741						0.571
Lateral amygdala	0.644		.600				
Ventricles	–0.616						
Dorsal CA3	–0.568						
Cortex	0.561						
Corpus callosum		0.907					
Pons		–0.847					
Dentate gyrus		0.842					
Ventral hippocampus		0.774					
Striatum		0.611					
Periaqueductal gray		0.610				0.532	
Ventral CA2			0.904				
Dorsal hippocampus			0.790				
Ventral CA3			0.789				
Ventral CA1		0.508	0.762				
Dorsal CA1			0.746				
Midbrain				0.919			
Thalamus				0.828			
White matter				0.809			
Hippocampus				–0.647			
Medulla				–0.541	.519		
Olfactory					–0.916		
Cerebellum					0.801		
Pituitary						0.932	
Infralimbic cortex							0.924
% variance explained = 91.9	29.4	22.6	16.3	9.3	7.9	5.7	3.9
Eigenvalues	0.039	0.030	0.021	0.012	0.010	0.007	0.005

Varimax rotation. Component loadings with an absolute value of >0.5 were suppressed. Loading values with an absolute value of >0.4 were suppressed. The coefficients were sorted according to size.